ELECTRONIC SUPPLEMENTARY INFORMATION

Confined methanol within InOF-1: CO$_2$ capture enhancement

Elí Sánchez-González,[†a] Paulo G. M. Mileo,[†b] J. Raziel Álvarez,[a] Eduardo González-Zamora,[c] Guillaume Maurin[*,b] and Ilich A. Ibarra[*,a]

[a] *Laboratorio de Fisicoquímica y Reactividad de Superficies (LaFReS), Instituto de Investigaciones en Materiales, Universidad Nacional Autónoma de México, Circuito Exterior s/n, CU, Del. Coyoacán, 04510, Ciudad de México, Mexico.*

E-mail: argel@unam.mx

[b] *Institut Charles Gerhardt Montpellier, UMR-5253, Université de Montpellier, CNRS, ENSCM, Place E. Bataillon, 34095 Montpellier cedex 05, France.*

E-mail: guillaume.maurin@univ-montp2.fr

[c] *Departamento de Química, Universidad Autónoma Metropolitana-Iztapalapa, San Rafael Atlixco 186, Col. Vicentina, Iztapalapa, C. P. 09340, Ciudad de México, Mexico.*

1. Materials and measurements

All reagents and solvents were used as received from commercial suppliers without further purification. Powder X-ray diffraction (PXRD) data were collected under ambient conditions on a Bruker AXD D8 Advance diffractometer operated at 160 W (40 kV, 40 mA) for Cu Kα_1 (λ= 1.5406 Å). Thermal gravimetric analysis (TGA) was performed under N_2 at a scan rate of 2 K min^{-1} using a TA Instruments Q500 HR analyser.

1.1 Sample preparation:

Acetone-exchanged InOF-1: Samples of as-synthesized InOF-1 soaking for 4 days in acetone.

Fully activated InOF-1: Acetone-exchanged samples of InOF-1 activated at 453 K and 10^{-3} bar or under a constant flow of N_2 (60 mL min^{-1}) for 2 h.

MeOH@InOF-1: Pre-adsorption of MeOH (saturation). Samples acetone-exchanged InOF-1 were placed in a quartz cell inside a BELPREP activation module and activated at 453 K for 2 hours. After that time, these samples were cooled down to room temperature (under N_2) and immediately immersed in methanol for 10 minutes. Then, the samples were recovered by filtration and kept in a desiccator for 8 hours. Later, this saturated samples with the MeOH were placed in a thermobalance (Q500 HR, from TA) and heated up from room temperature to 573 K (under N_2) in order to desorb all the alcohol molecules (MeOH) inside the micropores of InOF-1. The maximum load of MeOH was: 23 wt% for MeOH. These results were in good agreement with the MeOH alcohol isotherm.

Once the maximum amount of MeOH was established for InOF-1, more saturated samples were prepared. Then, different activation conditions (heating ramps to reach maximum temperatures, from 313 to 453 K) were used in order to desorb (in a controlled way) the amounts of MeOH that we determined. Thus, when saturated samples of MeOH were heated from room temperature to 443 K, with a ramp of 10 K min^{-1}, and immediately cooled down to 303 K (under N_2), the residual amount of the MeOH was approximately 2 wt%. This procedure was repeated 8 times in order to ensure the reproducibility of the experiment.
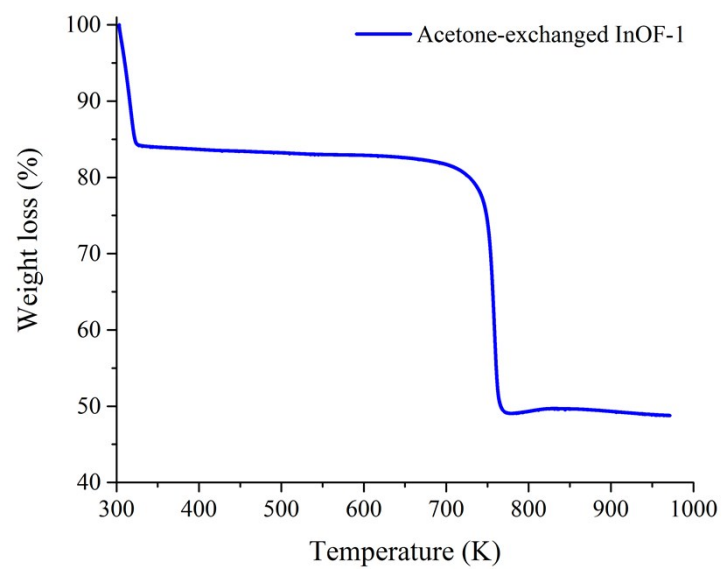
2. TGA plot

Fig. S1: TGA analysis of the acetone-exchanged InOF-1.

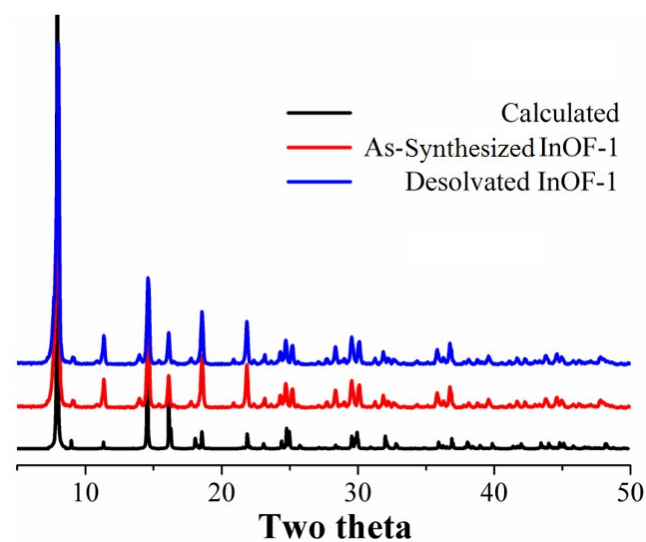## 3. Powder X-ray diffraction patterns of InOF-1

Fig. S2: PXRD patters of calculated (black), as synthesised (red) and calcined (blue) InOF-1.

4. Derivation of the isosteric enthalpy of adsorption for MeOH

The enthalpy of adsorption was calculated from the analysis of methanol adsorption isotherms using the isosteric method, Q_{st}, by fitting a virial-type equation to both 293 and 303 K methanol adsorption isotherms.[1] The following virial-type equation is used to fit both adsorption isotherms:[2]

$$\ln (n/p) = A_0 + A_1 n + A_2 n^2 ...$$
(1)

where p is pressure, n is amount adsorbed and A_0, A_1 etc. are virial coefficients. A_2 and higher terms can be ignored. A plot of $\ln(n/p)$ versus n should give a straight line at low surface coverage.[1]
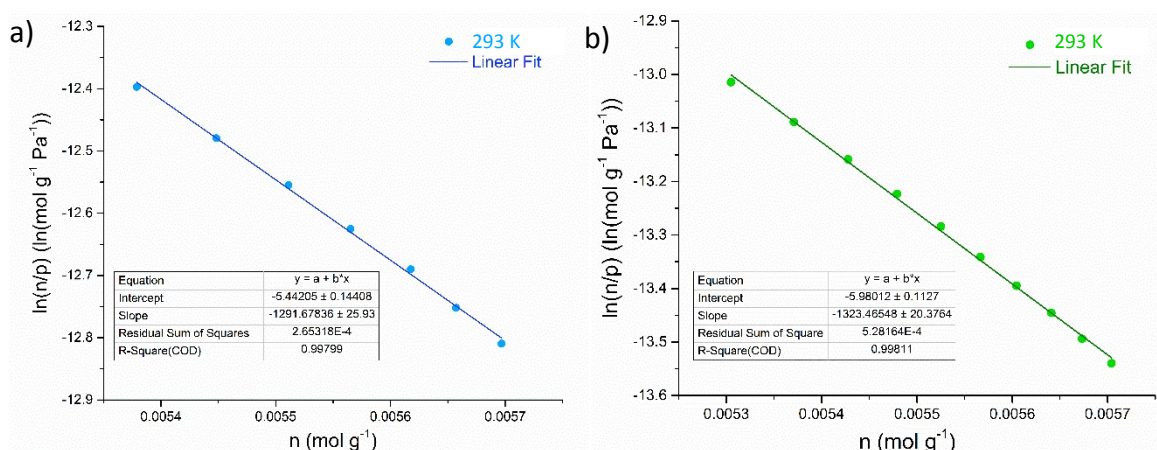
Fig. S3: Virial fitting plot for the adsorption of methanol on InOF-1 at 293 K (a) and 303 K (b).

The isoteric enthalpies of adsorption, Q_{st}, as a function of methanol uptake, was determined by using the Clausius-Clapeyron equation[2] (Fig. S4). The positive slope is indicative of homogeneous interactions due to, possibly, cooperative methanol-methanol interactions (*via* hydrogen bonding) rising with pressure increase.[3]
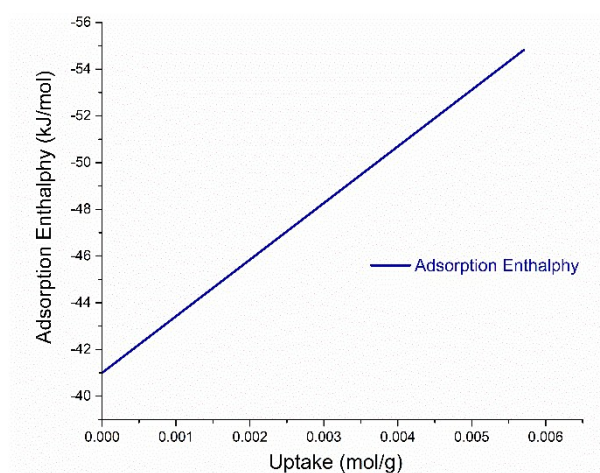

Fig. S4: Variation of adsorption enthalpy at low loading for InOF-1.

5. Computational details

The InOF-1 framework was modeled using the crystal structure reported previously[1]. The InOF-1 crystallizes in the space group $I4_122$ and is composed by binuclear $[In_2(\mu_2\text{-OH})]$ inorganic blocks bridged by $BPTC^{4-}$ ligands forming a 3-D framework with cylindrical channels with openings of 7.5 Å[4,5]. This structure was then geometry optimized at the Density Functional Theory (DFT) level maintaining its experimental unit cell parameters fixed. These calculations employed a PBE GGA functional[6,7] combined with the double numerical basis set containing polarization functions (DNP) on all atoms, as implemented in the Dmol[6] module[8,9]. The partial charges of each atom in the framework were calculated using the Mulliken charges (Table S1). The respective atom types are provided in Fig. S5.
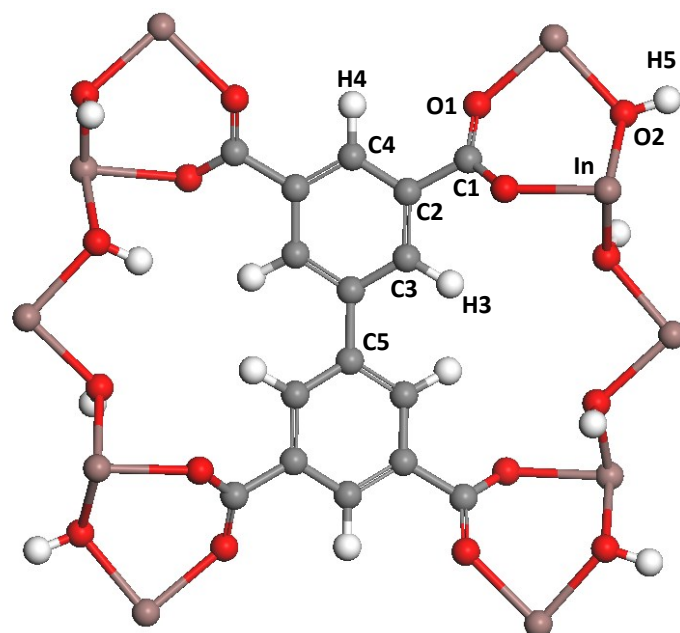

Fig. S5: Representative cluster of the InOF-1 and its atom types.

As mentioned in the main text, periodic Density Functional Theory calculations using the aforementioned specifications were performed to geometry optimize the CO_2@InOF-1 and MeOH@InOF-1 structures starting with the crystal structure of the empty InOF-1. We considered for both CO_2 and MeOH the loading explored experimentally, *i.e.* 5.2 wt% and 2 wt% respectively.

Monte Carlo simulations in the NVT ensemble were further carried out at 303 K to predict the adsorption behavior of the CO_2 and methanol in the InOF-1 framework. The simulation box was made of 8 conventional unit cells ($2 \times 2 \times 2$) maintaining the atoms of the MOF framework fixed in their initial positions. Short-range dispersion forces described by

Lennard-Jones (LJ) potentials were truncated at a cut-off radius of 12 Å while the Ewald summation method was used to calculate the Coulombic contribution. For each state point, 2×10^8 Monte Carlo steps following 10^7 equilibration steps were used. The energy of interaction in the system were tracked by energy histograms.

The same number of molecules experimentally observed at 1 bar and 303 K were modelled by NVT for the binary mixture CO_2/CH_3OH (5.4 / 2.0 wt%) as well as for the single component systems of CO_2 (5.2 wt.%) and CH_3OH (2.0 wt%).

The interactions between the InOF-1 and the guest molecules were modeled using a van der Waals 6-12 LJ contribution and a Coulombic term. The LJ parameters for the atoms of the organic linker were taken from the generic force field DREIDING.[10] The In(III) ions are considered as not polarizable and their LJ contributions are immersed in those provided by the μ_2-OH groups. The same methodology was already employed in the literature for several MOFs.[11]

Table S1: LJ parameters and atomic partial charges for the InOF-1 framework and the CO_2 and CH_3OH molecules.

Atom type	σ (Å)	ε (K)	Charge (e)
Framework			
C1	3.473	47.856	0.5231
C2	3.473	47.856	0.0041
C3	3.473	47.856	-0.1363
C4	3.473	47.856	-0.1088
C5	3.473	47.856	0.0576
O1	3.033	48.158	-0.5625
O2	3.118	92.123	-0.8089
H3	2.847	7.649	0.1362
H4	2.846	7.649	0.1611
H5	2.571	0.000	0.3136
In	3.976	0.000	1.5812
Methanol			
C_{CH3}	3.475	80.516	-0.0930
H_{CH3}	2.446	19.148	0.1000
O_{OH}	2.860	114.63	-0.4320
H_{OH}	-	-	0.2250
CO_2			
O_{CO2}	3.033	80.507	-0.3256
C_{CO2}	2.757	28.129	+0.6512

The CO_2 molecules were described as a 3 site-model. Their mutual interactions were modeled by the EPM2 model,[12] where both the LJ and charge sites are centered in the oxygen and carbon atoms. The methanol molecules were described by a flexible all-atom model[13] optimized to capture its interactions with the extra-framework cations in zeolites.

6. Computational results

The optimization of the MeOH@InOF-1 and CO_2@InOF-1 frameworks at the DFT level revealed that both MeOH and CO_2 interact preferentially with the μ_2-OH groups of the solid. For the methanol molecules, this interaction involves an interacting distance of 1.90 Å where the hydroxyl groups of the MeOH act as acceptor for the hydrogen from the μ_2-OH groups. Meanwhile, for the CO_2 molecules this preferential interaction occurs between the oxygen of the CO_2 molecules and the hydrogens of the μ_2-OH groups at a much longer distance about 2.95 Å.
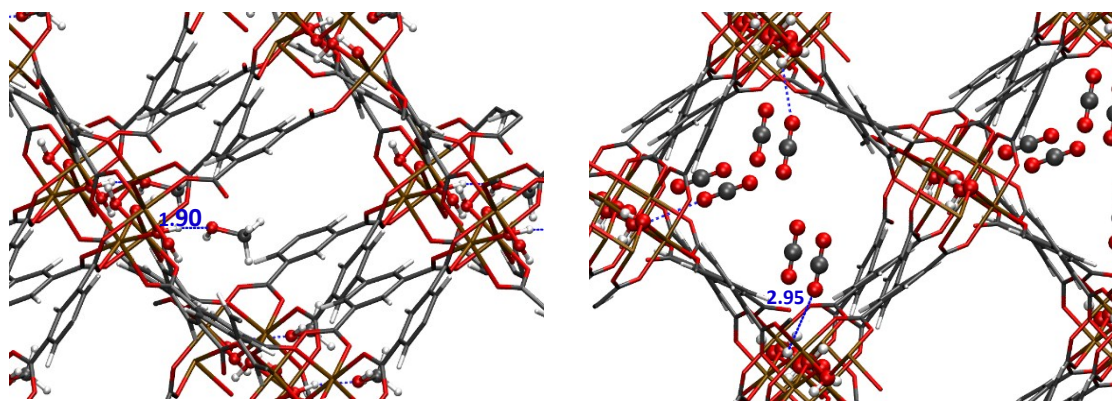

Fig. S6: DFT-optimized structures for the MeOH@InOF-1 (a) and CO_2@InOF-1 (b), showing the preferential adsorption of the guest towards the hydroxyl groups.

The stronger interaction between the μ_2-OH groups and the methanol molecules can also be observed from the Monte Carlo simulations, observing, for instance, the much more localized center of mass (COM) distribution of the MeOH molecules at the vicinities of the hydroxyl groups of the InOF-1 compared to the much more scattered COM distribution of the CO_2 molecules in the pores of the framework (Fig. S7).
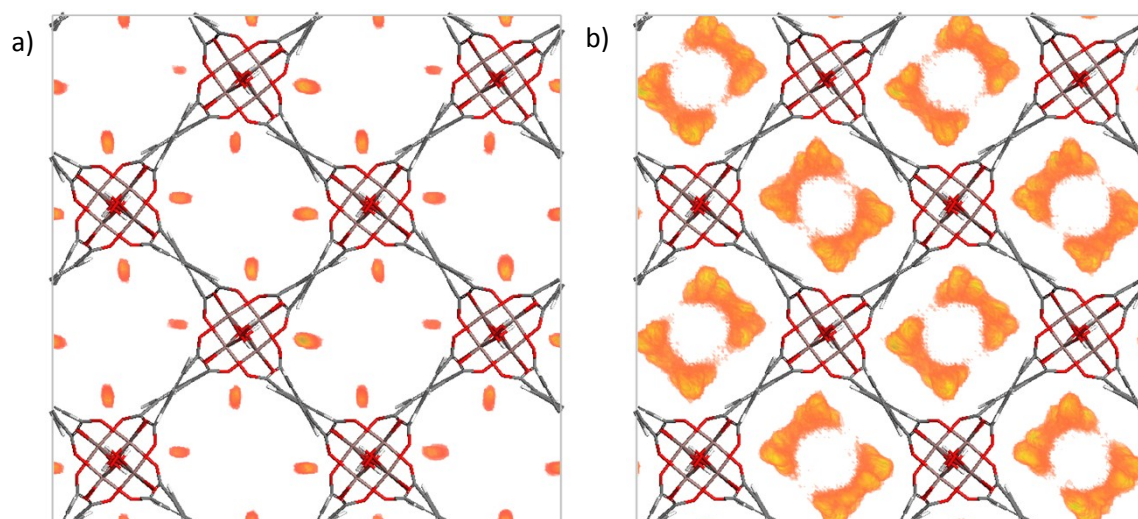
Fig. S7: Center of mass distribution for the single-component MC NVT calculations of the MeOH (a) and CO_2 (b) adsorption in the InOF-1.

As seen in the energy histograms of the single-component and mixture MC calculations of CO_2 and MeOH, there is only a minor shift (from -21 kJ mol^{-1} to -23 kJ mol^{-1}) in the interacting energy involved in the CO_2 adsorption with the presence of 2 wt% of methanol. Therefore, as discussed in the main text, the enhancement of the adsorption of CO_2 in presence of methanol is rather associated with the reduction of the apparent porosity in the framework rather than an enhancement of the crossed interactions between the two guest molecules.
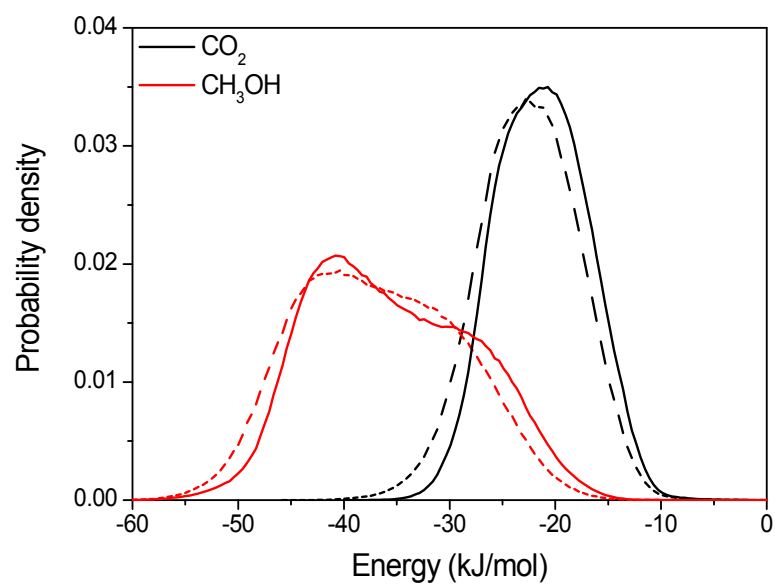
Fig. S8: Energy histograms from MC calculations of CO_2 (black plots) and MeOH (red plots) as single components (full lines) and in a mixture of 5.4 and 2.0 wt% respectively (dashed lines).

References

1. I. A. Ibarra, S. Yang, X. Lin, A. J. Blake, P. J. Rizkallah, H. Nowell, D. R. Allan, N. R. Champness, P. Hubbderstey and M. Schröder, *Chem. Commun.*, 2011, **47**, 8304.

2. M. P. Suh, H. J. Park, T. K. Prasad and D.-W. Lim, *Chem. Rev.*, 2012, **112**, 782.

3. A. J. Nuñez, M. S. Chang, I. A. Ibarra and S. M. Humphrey, *Inorg. Chem.*, 2014, **53**, 282.

4. J. Qian, F. Jiang, D. Yuan, M. Wu, S. Zhang, L. Zhang and M. Hong, *Chem. Commun.*, 2012, **48**, 9696.

5. R. A. Peralta, A. Campos-Reales-Pineda, H. Pfeiffer, J. R. Álvarez, J. A. Zárate, J. Balmaseda, E. González-Zamora, A. Martínez, D. Martínez-Otero, V. Jancik and I. A. Ibarra, *Chem. Commun.*, 2016, **52**, 10273–10276.

6. J. P. Perdew, K. Burke and M. Ernzerhof, *Phys. Rev. Lett.*, 1996, **77**, 3865–3868.

7. J. P. Perdew, K. Burke and M. Ernzerhof, *Phys. Rev. Lett.*, 1997, **78**, 1396.

8. B. Delley, *J. Chem. Phys. Addit. Inf. J. Chem. Phys. J. Homepage*, , DOI:10.1063/1.458452.

9. B. Delley, *J. Chem. Phys.*, 2000, **113**, 7756–7764.

10 S. L. Mayo, B. D. Olafson, W. a G. Iii, E. Eb and E. a E. T. El, *J. Phys. Chem.*, 1990, **101**, 8897–8909.

11. Q.Y. Yang, S. Vaesan, M. Vishnuvarthan, F. Ragon, C. Serre, A. Vimont, M. Daturi, G. De Weireld, G. Maurin, *J. Mater. Chem.*, 2012, 22, 10210.

12. J. G. Harris and K. H. Yung, *J. Phys. Chem.*, 1995, **99**, 12021–12024.

13. D. F. Plant, G. Maurin and R. G. Bell, *J. Phys. Chem. B*, 2007, **111**, 2836–2844.